SEARCH FOR CHEMISORBED HCO: THE INTERACTION OF FORMALDEHYDE, GLYOXAL AND ATOMIC HYDROGEN + CO WITH RH

NATIONAL BUREAU OF STANDARDS,
WASHINGTON, DC. NATIONAL MEASUREMENT LAB

MAY 1981

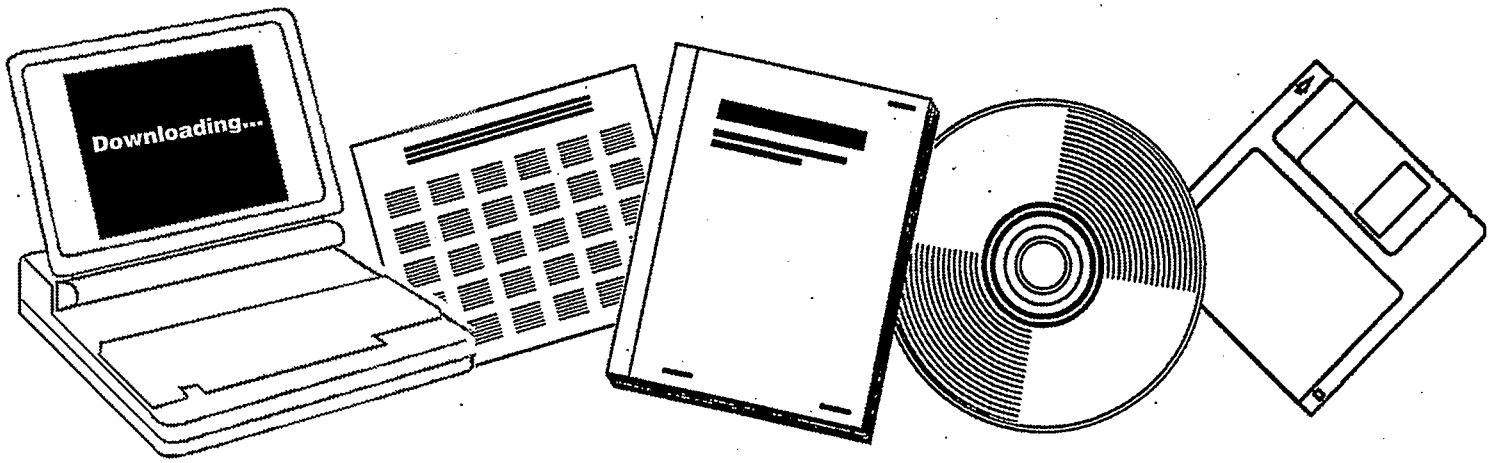

SEARCH FOR CHEMISORBED HCO: THE INTERACTION OF FORMALDEHYDE, GLYOXAL AND ATOMIC HYDROGEN + CO WITH Rh

J. T. Yates, Jr.

and

R. R. Cavanagh*+

Surface Science Division

National Bureau of Standards

Washington, D.C. 20234

*NRC-NBS Postdoctoral Research Associate 1979-1981 +Present address: Molecular Spectroscopy Division, National Bureau of Standards, Washington, DC 20234

SECURITY CLASSIFICATION OF THIS PAGE (When Data Entered)

REPORT DOCUMENTATION PAGE

READ INSTRUCTIONS BEFORE COMPLETING FORM

1. REPORT NUMBER: Technical Report No. 22
2. GOVT ACCESSION NO.: AD-A099 970
3. RECIPIENT'S CATALOG NUMBER:

4. TITLE (and Subtitle): Search for Chemisorbed HCO: The Interaction of Formaldehyde, Glyoxal and Atomic Hydrogen + CO with Rh
5. TYPE OF REPORT & PERIOD COVERED:
6. PERFORMING ORG. REPORT NUMBER:

7. AUTHOR(s): J. T. Yates, Jr. and R. R. Cavanagh

8. CONTRACT OR GRANT NUMBER(s): N0014-81-F-0008 Mod. No. P00001

9. PERFORMING ORGANIZATION NAME AND ADDRESS: Surface Science Division, National Bureau of Standards, Washington, DC 20234

10. PROGRAM ELEMENT, PROJECT, TASK AREA & WORK UNIT NUMBERS:

11. CONTROLLING OFFICE NAME AND ADDRESS:

12. REPORT DATE: May, 1981
13. NUMBER OF PAGES:

14. MONITORING AGENCY NAME & ADDRESS (if different from Controlling Office):

15. SECURITY CLASS. (of this report): Unclassified
15a. DECLASSIFICATION/DOWNGRADING SCHEDULE:

16. DISTRIBUTION STATEMENT (of this Report): Approved for Public Release; Distribution Unlimited

17. DISTRIBUTION STATEMENT (of the abstract entered in Block 20, if different from Report):

18. SUPPLEMENTARY NOTES: Preprint; to be published in Journal of Catalysis

19. KEY WORDS (Continue on reverse side if necessary and identify by block number): Chemisorption; formaldehyde; formyl; glyoxal; Rh.

20. ABSTRACT (Continue on reverse side if necessary and identify by block number): Transmission infrared spectroscopy has been used to search for the chemisorptive-stabilization of formyl (HCO) on Al_2O_3-supported Rh surfaces. Formaldehyde (H_2CO) and glyoxal ($(HCO)_2$) have been used as potential sources of HCO. In addition, chemisorbed CO on Rh has been treated with atomic deuterium in an attempt to produce DCO. None of these routes have led to spectroscopically detectable levels of formyl adsorption at temperatures near or above 100K. These results suggest that the formyl intermediate may not be a stable surface species on Rh in CO-hydrogenation chemistry.

DD FORM 1 JAN 73 1473 EDITION OF 1 NOV 65 IS OBSOLETE S/N 0102-014-6601

Unclassified 410 605

SECURITY CLASSIFICATION OF THIS PAGE (When Data Entered)

13

SEARCH FOR CHEMISORBED HCO: THE INTERACTION OF FORMALDEHYDE, GLYOXAL AND ATOMIC HYDROGEN + CO WITH Rh

J. T. Yates, Jr.

and

R. R. Cavanagh

Surface Science Division

National Bureau of Standards

Washington, D.C. 20234

ABSTRACT

Transmission infrared spectroscopy has been used to search for the chemisorptive-stabilization of formyl (HCO) on Al_2O_3-supported Rh surfaces. Formaldehyde (H_2CO) and glyoxal $(HCO)_2$ have been used as potential sources of HCO. In addition, chemisorbed CO on Rh has been treated with atomic deuterium in an attempt to produce DCO. None of these routes have led to spectroscopically detectable levels of formyl adsorption at temperatures near or above 100K. These results suggest that the formyl intermediate may not be a stable surface species on Rh in CO-hydrogenation chemistry.

SEARCH FOR CHEMISORBED HCO: THE INTERACTION OF FORMALDEHYDE, GLYOXAL AND ATOMIC HYDROGEN + CO WITH Rh

J. T. Yates, Jr. and R. R. Cavanagh

Surface Science Division

National Bureau of Standards

Washington, D.C. 20234

I. INTRODUCTION

Mechanistic details of the catalytic production of CH_4 and larger hydrocarbons from $H_2(g)$ + CO(g) have been the subject of much recent speculation. Experimental studies in coupled high pressure/ultra high vacuum systems have demonstrated the active role of surface carbon (or CH_x species) on Ni single crystals in such reactions. (1) The capacity to form CH_4 from the reaction with $H_2(g)$ of CO-produced surface carbon indicates that CO dissociation is a compatible first step in the catalytic reaction pathway to CH_4. Further studies of various types have supported the CO dissociation mechanism on Ru (2-4). Similar conclusions have been reached regarding C formation from CO on polycrystalline Rh surfaces (5), and in particular on stepped Rh single crystals (6,7), although the efficiency of CO dissociation processes on Rh is a controversial issue at present (7).

Contrary to a model involving dissociative CO chemisorption as the primary elementary step in the catalytic formation of hydrocarbons, mechanisms involving the hydrogenation of CO to form various intermediates such as HCO (ads) or HCOH (ads) have also been widely discussed in the recent literature, as exemplified in a review article by Muetterties and

Stein (8), as well as in earlier reviews (9). In addition, experimental observations which detected small quantities of CH_4 produced from H_2CO chemisorption on Ru(110) (10) and on W(100) and W(111) (11, 12) have lent support to the alternate model, in which species like adsorbed formyl, HCO (ads), are postulated to be involved in the catalytic synthesis of CH_4 from CO and H_2. While the exact role played by these species during a chemical reaction is not known, the synthesis of model inorganic compounds containing such functional groups clearly demonstrates their existence (13).

The work to be discussed in this paper addresses the question of the stabilization of species like HCO (ads) on an Al_2O_3-supported Rh surface. We have employed molecules such as H_2CO and $(HCO)_2$ as adsorbates at 100 K. Transmission infrared spectroscopy was used to search for intermediates in the catalytic decomposition of these molecules as the surface was warmed to 340 K. In addition, atomic deuterium was employed as a reactant with chemisorbed CO on Rh in an attempt to produce DCO (ads).

The combination of low temperature adsorption techniques with infrared spectroscopy on supported metal systems is a potentially promising method for trapping and observing such transient reaction intermediates. Temperature dependent surface binding state distributions between 77 and 300K are well known on single crystal substrates from investigations using a variety of surface sensitive spectroscopies, yet rarely have such species been studied using the infrared transmission technique. The combination of low temperature methods with model adsorbate systems provides a unique opportunity to prepare, isolate, and study various proposed reaction intermediates.

II. EXPERIMENTAL

Complete details of the sample preparation, vacuum system, and spectrometer have appeared elsewhere (14, 15). In brief, a solution of Rh^{III} ions was prepared by dissolving $RhCl_3 \cdot 3H_2O$ in water. This mixture was then used to impregnate an amount of Al_2O_3 (DeGussa-C)** such that the weight percentage of rhodium would be 2.2%. Acetone was then added to the solution (10:1 = acetone:water). This slurry was sprayed onto a CaF_2 plate held at 350K causing flash evaporation of solvents. Typical deposit loadings of 11mg/cm^2 were obtained. The deposited sample was then mounted in the ultrahigh vacuum infrared cell, outgassed at 425K, reduced in H_2 at 425K, and further outgassed at 475K for eight hours. All infrared spectra were recorded on a Perkin Elmer Model 180 Infrared Spectrometer**.

$H_2CO(g)$ was prepared by heating paraformaldehyde in a gas generator at 350K, passing the gas through a glass trap at 195K, and directly admitting the $H_2CO(g)$ to the stainless steel manifold. The purity of the $H_2CO(g)$ obtained by this method is well established (11).

$(CHO)_2(g)$ was obtained using established literature methods (16). A mixture of P_2O_5 and trimeric glyoxal dihydrate $(C_2H_2O_2)_3 \cdot (2H_2O)$ (1:1) was placed in a glass system similar to that used for the formaldehyde generator. The generator was evacuated and the glass trap immersed in liquid nitrogen. While pumping on the generator/trap, the mixture was gently heated. In addition to the evolution of non-condensible gases, both yellow crystals and white crystals appeared in the glass trap. The $P_2O_5/(C_2H_2O_2)_3 \cdot (2H_2O)$ vessel was isolated from the trap, and the trap was brought to 195K, at which time the evolution of additional non-

condensibles and the disappearance of the white crystals was noted. The remaining yellow crystals were further purified by a freeze-pump-thaw cycle. The pressure of an aliquot of vapor obtained upon warming from this purified sample was found to be stable in the stainless steel manifold to 0.1% over several minutes.

The generation of deuterium atoms was achieved with a thermal source operating in a D_2 atmosphere. In these experiments, a high temperature tungsten filament was operated inside the infrared cell (see Figure 1). The adsorbent was shielded from radiation from the filament by means of a baffle arrangement. The D_2 gas phase pressure in the range 0.2 torr-0.01 torr was monitored with a capacitance manometer as a function of filament temperature; we observed the initiation of a continuous pressure drop at the onset of D atom generation. This is presumably due to interaction of D atoms with the cell walls or the sample.

Due to the location of the thermocouple on the copper sample holder rather than within the sample itself, there is some uncertainty as to the exact temperature of the specimen. Rather than attempt to correct for this error, the temperatures given refer simply to the temperature of the copper support assembly.

III. INTERACTION OF FORMALDEHYDE WITH Al_2O_3 AND WITH Rh/Al_2O_3.

A. H_2CO Adsorbed on Al_2O_3

A Rh free sample of Al_2O_3 weighing 58mg was prepared as described in the experimental section. This sample was then cooled to $\sim$ 100K and exposed to 6×10^{19} molecules of $H_2CO(g)$. This dose of H_2CO corresponded

to ~ 1 molecule per 10$\mathring{A}^2$ of Al_2O_3 surface area. Following measurement of the infrared spectrum, the surface was warmed in a stepwise fashion to 300K and spectral developments were followed, as shown in Fig. 2. Finally, at 300K, the cell was evacuated and spectrum 2e was recorded.

At 160K, a distinct feature due to physisorbed H_2CO develops near 1700cm^{-1}; upon warming the dosed cell to 300K, the 1700cm^{-1} feature has diminished in intensity, while additional absorbance due to $H_2CO(g)$ develops near 1750cm^{-1}. After evacuation at 300K, there is little evidence for either feature. However, new features which appear at 1591cm^{-1}, 1392cm^{-1} and 1372cm^{-1} persist upon evacuation. These three features are in excellent agreement with those reported for formate production from CH_3OH decomposition on Al_2O_3 [1597cm^{-1}; 1394cm^{-1}; 1377cm^{-1}] (17).

The region between 2700cm^{-1} and 2000cm^{-1} was carefully examined during this experiment, since this is the region in which the H-C stretching frequency for HCO(ads) would be expected. The only additional feature which appeared was a broad weak feature near 2040cm^{-1} (6% of the 1700cm^{-1} peak intensity). This feature disappears upon evacuation at 300K. Table I summarizes the observed spectral features in this series of measurements.

B. H_2CO Adsorbed on Rh/Al_2O_3

A 61 mg sample containing 2.2% Rh was prepared. Following cooling to 100K, the sample was exposed to 8 x 10^{18} molecules of $H_2CO(g)$. From previous experiments we know that the chemisorptive capacity of this Rh/Al_2O_3 sample for CO(g) should be ~ 1.1 x 10^{19} CO molecules (18).

The spectral development as a function of temperature is shown in Fig. 3. The spectral feature observed near 1700cm^{-1} at 160K can be associated with H_2CO physisorbed on Al_2O_3, as seen for pure Al_2O_3 in Fig. 2. As the Rh/Al_2O_3 sample is warmed, the development of additional spectral features between 2100 and 1800cm^{-1} is apparent. At 230K spectral features at 1860, 2021, 2045 and 2088cm^{-1} are observed as well as H-C stretching modes at $\sim$ 2910 and $\sim$ 2980cm^{-1}. An additional weak feature at $\sim$ 2790cm^{-1} is also observed.

Previous work has shown that the 1860cm^{-1} feature can be assigned to bridge-bonded CO (14, 19, 20) on Rh crystallite sites. For pure CO adsorption, features in the 2000-2100cm^{-1} region have been assigned to terminal CO species on Rh crystallites [$\sim$ 2050-2070cm^{-1}] (14) and to $Rh(CO)_2$ species produced on isolated Rh sites [2101; 2031cm^{-1}](14,18). The features at 2088cm^{-1} and 2021cm^{-1}, as produced by $H_2CO(g)$ adsorption, are $\sim$ 10cm^{-1} lower in wavenumber than the corresponding features produced by CO(g) adsorption, in agreement with earlier observations for H_2CO adsorption on Rh/Al_2O_3 (21). This 10cm^{-1} shift will be discussed in section III.C.

It should be noted here that the intensity of absorbance in the 2100 to 1800cm^{-1} region for all of these features derived from $H_2CO(g)$ adsorption is much lower than expected for full CO coverage. This observation is confirmed also from the experiment shown in spectrum 3d where the $H_2CO(g)$ was pumped from the cell and $^{12}CO(g)$ was introduced. The significant increase in absorbance at 1860, 2020, 2050, and 2093cm^{-1} indicates the presence of active Rh sites for CO chemisorption in spite of the high dose of $H_2CO(g)$.

C. Perturbation of Rh-Chemisorbed CO Species by Adsorbates on the Al_2O_3 Support.

It is possible that small spectral shifts for chemisorbed CO on Al_2O_3-supported Rh could be due to interactions with adsorbed CO caused by adsorption of other molecules on the Al_2O_3 support, in much the same fashion as observed in matrix isolation infrared spectroscopy for changes in the matrix. Two experiments were carried out in order to check this point:

1. H_2O + CO/Rh/Al_2O_3.

A Rh/Al_2O_3 sample was exposed to H_2O(g) at 0.5 torr pressure. Increased absorbance was observed in the OH stretching region between 3700 and 3000cm^{-1} and a feature due to H_2O adsorption on Al_2O_3 is observed in the HOH bending region near 1620cm^{-1}. Only minor changes in CO-derived spectral features on Rh were observed when the evacuated sample was subsequently exposed to CO(g); spectral features at 2098, 2053, 2027 and 1860cm^{-1} were produced. This corresponds to an approximately 2-3cm^{-1} decrease in wavenumber for the doublet from values of 2101 and 2031cm^{-1} observed on H_2O free surfaces.

2. H_2CO + CO/Rh/Al_2O_3.

In a separate experiment, a 2.2% Rh sample was saturated with ^{13}CO and evacuated (see Fig. 4) resulting in ^{13}CO features at 2053, 2035,

1987, and 1825cm^{-1}. This sample was subsequently exposed to a saturation coverage of H_2 ^{12}CO [see Fig. 4(c)]. The features previously associated with the formation of formates on the Al_2O_3 are clearly present. In addition, the two sharp IR peaks associated with ^{13}CO bound to Rh as $Rh(CO)_2$ were observed to shift to lower wavenumber by 10cm^{-1} to 2042 and 1975cm^{-1}. Introduction of additional H_2CO resulted in a further shift of the ^{13}CO features. The significant shift in the ^{13}CO features, and the absence of infrared evidence for ^{12}CO-^{13}CO exchange demonstrates a strong support perturbation of the Rh-bound CO modes attributable to the presence of oxide-bound species derived from H_2CO.

IV. Interaction of Glyoxal with Al_2O_3 and with Rh/Al_2O_3.

A. $(HCO)_2$ Adsorbed on Al_2O_3.

In Fig. 5, a 55mg sample of Al_2O_3 was exposed to 4 x 10^{19} $(HCO)_2(g)$ molecules at 100K and then warmed. Infrared spectra as a function of sample temperature are shown. Spectrum 5(a) indicates the presence of very little adsorbate on the Al_2O_3, presumably because of condensation of the $(HCO)_2(g)$ on cooler regions of the sample support assembly. Upon warming to 190K, two predominant peaks at 1720cm^{-1} and 1748cm^{-1} are observed as $(HCO)_2$ transfers to the Al_2O_3. Between 235K and 275K, an inversion of relative intensity occurs as the intensity of the 1720cm^{-1} feature decreases while the intensity of the 1748cm^{-1} feature increases. The only other features observed between 3200cm^{-1} and 1400cm^{-1} were bands at 2930cm^{-1} and 2840cm^{-1}. There are small changes in the relative

intensity of these two bands during sample warming, but both bands persist upon evacuation of the cell. The behavior observed on warming the Al_2O_3 surface from 190K to 305K is not observed to be reversible upon subsequent cooling back to 100K. The presence of an intense feature at 1748cm^{-1} upon evacuation at 305K is in distinct contrast to the behavior observed for H_2CO on Al_2O_3 (Fig. 2), where irreversibly adsorbed formate species are produced.

B. $(HCO)_2$ Adsorbed on Rh/Al_2O_3:

The adsorption of $(HCO)_2$(g) on a 2.3% Rh sample weighing 90mg is shown in Fig. 6. By comparison with data obtained for pure Al_2O_3 (Fig. 5) it may be seen that the behavior in the 1700-1800cm^{-1} region and in the 2800-3000cm^{-1} region is very similar, suggesting that these spectral features are unrelated to the interaction of $(HCO)_2$ with Rh. At temperatures above 190K, new infrared features in the 1800-2100cm^{-1} region are observed due to the interaction of $(HCO)_2$ with Rh. Comparing glyoxal spectrum 5(c) with formaldehyde spectrum 3(c) suggests that the infrared spectrum of the species present on the Rh sites are very similar although relative intensities differ somewhat. Thus in each case we observe major bands at $\sim$2045 and $\sim$1860cm^{-1} similar to those observed for low coverages of CO(ads) on crystalline Rh sites (14,18). In addition small features at $\sim$2090cm^{-1} and $\sim$2020cm^{-1} are observed in both cases, indicative of formation of relatively small amounts of $Rh(CO)_2$ (14,18). It is observed that the intensities of all of these features due to $(HCO)_2$ adsorption is below that observed for CO(g) adsorption.

Subsequent CO exposure of the $(HCO)_2$-exposed Rh/Al_2O, sample at 300K causes full development of the expected features due to CO(ads) as shown in Fig. 6(e). Thus, exposure to a large dose of $(HCO)_2(g)$ does not cause full occupancy of all Rh sites capable of CO adsorption. Similar behavior was also observed with the H_2CO adsorbate.

V. INTERACTION OF MOLECULAR AND ATOMIC HYDROGEN WITH CO ADSORBED ON Rh.

In earlier work, the exposure of dispersed Rh on Al_2O_3 to a mixture of $H_2(g)$ and CO(g) at 300K resulted in comparable infrared spectra to that obtained for pure CO exposures (21). In addition, LEED studies and thermal desorption studies have indicated that repulsive CO(ads)-H(ads) interactions occur on Rh(111), leading to a lowering of the desorption energy for H(ads) (22). Thus it might be expected that the competition between $H_2(g)$ and CO(g) for Rh adsorption sites would favor CO if the temperature is sufficiently high, permitting rapid H_2 desorption following addition of CO.

In Figure 7, a 2.2% Rh/Al_2O_3 sample was first saturated at 310K with CO, giving the infrared spectrum shown in 6(a), which is typical for pure CO adsorption (14, 15, 18, 21). The CO was pumped away and the CO-saturated sample was exposed to $D_2(g)$ at 102 torr and 310K. Following 19 hours exposure spectrum 6(b) was obtained. There is some loss of intensity at 2101cm^{-1} and at 2031cm^{-1} corresponding to a decrease in the concentration of $Rh(CO)_2$ species. Similar effects have been observed during reversible thermal desorption of CO from these surfaces (14). In addition, slight exchange of Al_2O_3-bound hydrogen (AlOH) with deuterium

is observed by the appearance of enhanced intensity in a broad band with its peak maximum at 2650cm^{-1}. This deuterium exchange at 310K occurs only with the involvement of Rh sites for chemisorptive D_2 dissociation followed by D migration on the Al_2O_3 and has been studied previously (23). An additional exposure to D_2(g) at 282 torr resulted in only slight changes in intensity but yielded no additional infrared features. The cell was then evacuated, CO(g) was added to resaturate the Rh surface, and the CO was then evacuated while cooling to 90K. The cell was then filled with 0.1 Torr of D_2(g) and the tungsten atomization filament was turned on to bombard the surface with atomic D. A substantial drop in D_2(g) pressure occurred, and the substrate temperature increased to 170K. Infrared spectra corresponding to various amounts of atomic D bombardment of the surface are shown in Figure 7(c) and 7(d). A total exposure to $\sim 2 \times 10^{19}$ D atoms corresponds to spectrum 7(d). No new spectral features were observed during this treatment.

V. DISCUSSION

A. The Infrared Spectrum of the HCO Ligand

Using matrix isolation techniques, the infrared spectrum of HCO has been measured in a CO matrix at 14-20K (24,25). It exhibits a C=O stretching mode at 1860cm^{-1}, an intense C-H stretching mode at 2488cm^{-1} (25), and a H-C=O bending vibration at 1090cm^{-1} (24,25). HCO is characterized by a weak C-H bond and by a corresponding high C=O stretching frequency (25,26). Synthesis of matrix isolated HCO is

achieved at low temperatures by the interaction of energetic (photolytically produced) H atoms with a CO matrix. In attempts to use thermalized H atoms reacting with CO in an Ar matrix, no reaction has been observed (27).

When HCO is bound as a ligand to transition metal atoms, the C=O stretching frequency is usually observed to shift downwards to 1600cm^{-1} and an increase of 100-200cm^{-1} in the CH stretching frequency is observed. A summary of information regarding characteristic frequencies for the HCO moiety is given in Table II.

Based on Table II it would seem appropriate to search for HCO (ads) infrared features in the range 1500-1800cm^{-1} (ν_{C-O}) and in the range 2500-2700cm^{-1} (ν_{H-C}). The bending vibration below 1100cm^{-1} is in an experimentally difficult region in this work due to strong absorption by the Al_2O_3 support.

B. Lack of Evidence for Production of HCO (ads) from either H_2CO or $(HCO)_2$ on Rh/Al_2O_3.

By comparison of the infrared spectra (Fig. 2 and 3) for H_2CO on Al_2O_3 and on Rh/Al_2O_3, it is evident that under no condition of temperature utilized here is there evidence for additional absorption bands on the Rh/Al_2O_3 surface in either the 1500-1800cm^{-1} region or the 2500-2700cm^{-1} region. On this basis we can be confident that HCO (ads) is not produced at a spectroscopically detectable level on Rh from H_2CO adsorbate.

The same comparison may be made for $(HCO)_2$ adsorbate. Here too, no extra absorption bands related to HCO (ads) species on Rh are detected in the 1500-1800cm^{-1} region or the 2500-2700cm^{-1} region. Thus $(HCO)_2$ is also not a favorable source of HCO (ads) on an Al_2O_3-supported Rh surface.

C. Atomic Deuterium + CO (ads). Lack of Evidence for DCO (ads) by this Route.

Although expected to be an unlikely route to DCO (ads) formation, a chemisorbed CO layer on Rh was exposed to thermalized D atoms at ~170K. The D-CO stretching frequency would be expected at about 2000cm^{-1} for DCO (ads). The DC=O stretching frequency would be expected between 1800cm^{-1} and about 1550cm^{-1} (25) [See also Table II]. Although the 2000cm^{-1} region is strongly overlapped by chemisorbed CO intensity, there is no evidence in either region for additional absorption due to the formation of DCO (ads) species.

D. Interaction of H_2CO and $(HCO)_2$ with Rh/Al_2O_3.

The similarity in the infrared spectra for species produced on Rh from H_2CO and from $(HCO)_2$ is evident by comparison of Figures 3 and 6. On the basis of comparisons with intensities achieved for pure CO adsorption, it is clear that both H_2CO and $(HCO)_2$ yield appreciable quantities of both terminal-CO and bridged-CO species. These species are present on the crystalline Rh sites described previously (14,18). The $Rh(CO)_2$ species are not strongly populated by exposure to H_2CO or $(HCO)_2$, but

may be filled by subsequent CO adsorption. A previous model suggested to explain this lack of production of $Rh(CO)_2$ from H_2CO adsorption postulated the formation of H-Rh-CO species from H_2CO (21). This picture was based on the observation of a shifted $Rh(CO)_2$ doublet when H_2CO+CO were adsorbed. The work reported here in section III.C. has shown that this shift was in fact due to interaction of the $Rh(CO)_2$ with adsorbates produced by H_2CO on the Al_2O_3 support. We now believe that neither H_2CO nor $(HCO)_2$ decompose appreciably on the isolated Rh sites.

Two factors may be responsible for this low reactivity of the isolated Rh sites:

(1) both H_2CO and $(HCO)_2$ require multiple sites to dissociatively chemisorb

(2) the special electronic character of isolated Rh sites prohibits dissociative chemisorption of H_2CO and $(HCO)_2$. There is evidence that the isolated sites are in fact Rh^+ species (18). Primet and Garbowski have assigned these sites as Rh(I) based on UV-visible absorption spectral studies of a Rh-Na zeolite (30).

E. Interaction of H_2CO with Al_2O_3.

Upon warming the H_2CO/Al_2O_3 sample from 100K to 300K, several distinct transitions occur. By 160K, the intensity of the 3730 and 3660cm^{-1} features due to free OH on Al_2O_3 was decreased by a factor of two, while the broad hydrogen bonded OH feature near 3500cm^{-1} has increased in intensity significantly. Previous work on silica surfaces (31,32) has shown that free OH features can be shifted by as much as 350cm^{-1} to lower wavenumber due to interaction with R_2CO groups. We

therefore suggest that at 160K, evidence for a site specific interaction of H_2CO on Al_2O_3 exists.

Simultaneously, distinct features appear at lower wavenumber which indicate the presence of molecularly adsorbed H_2CO (see Table III). The observed shifts and/or multiple peaks observed for ν_5, ν_4, ν_3 and ν_2 could be attributed to either;

a) a single binding site on Al_2O_3 which reduces the symmetry of the adsorbed species from the gas phase symmetry of C_{2v}.

b) adsorption at a number of distinct binding sites.

Additional warming serves to clarify the situation. Once the sample has reached room temperature, all of the features observed at 200K (with the exception of the 1470cm^{-1} feature) have maximized in strength, and have begun to diminish. Three new features have also become apparent, dominating figure 2e at 1392, 1372 and 1594cm^{-1}. Greenler (17) has attributed these modes to formate (HCOO) formation from CH_3OH decomposition on Al_2O_3. Evacuation of the sample further reduces the intensity above 1700cm^{-1} and below 1350cm^{-1}. In most of the spectral regions of interest, it is not possible to make a meaningful measure of the loss of intensity, since formate modes and formaldehyde modes will be unresolved. For instance, in the C-H stretching region, as the conversion of H_2CO to formate occurs, the contributions from the formate C-H stretch (17b) would be expected to compensate for loss of formaldehyde C-H stretch absorption. However, the CH_2 deformation mode observed at 1470cm^{-1} is spectrally isolated from any formate modes. This feature neither shifts nor changes in intensity after the sample has reached 200K. This clearly indicates the presence of a site which

is stable for formaldehyde bonding between 200 and 310K. Thus, at least two sites exist for the binding of H_2CO to Al_2O_3. One site associated with the CH_2 mode at 1470cm^{-1}, and another site on which formaldehyde converts to formate.

F. Interaction of $(HCO)_2$ with Al_2O_3.

In the process of carrying out the control experiments with $(HCO)_2$ on Al_2O_3, an interesting temperature dependence was observed in the infrared spectra, as shown in Figure 5. At temperatures below about ~250K, the dominant carbonyl stretching feature is seen at 1720cm^{-1}; upon warming above 250K, the 1720cm^{-1} feature disappears and a 1748cm^{-1} feature is enhanced. The species corresponding to the 1748 cm^{-1} feature is involatile at 305K as shown in spectrum 5(e).

We assign the 1720cm^{-1} feature to monomeric $(HCO)_2$ adsorbed on Al_2O_3. For comparison $(HCO)_2$(g) exhibits a fundamental ν_{CO} of 1745cm^{-1} (35). $(HCO)_2$ may exist as a cis or trans isomer, but both isomers have been shown to exhibit a ν_{CO} within 1cm^{-1} of each other. Thus, the adsorption by Al_2O_3 of $(HCO)_2$ monomer is associated with a 25cm^{-1} <u>decrease</u> in ν_{CO}, compared to $(HCO)_2$(g). In this context, we have observed that <u>physisorbed</u> ^{13}CO on Al_2O_3 at 100K produces an absorption band at 2190cm^{-1}, or a shift to <u>higher</u> wavenumber of 13cm^{-1} from the gas value. This suggests that the monomer $(HCO)_2$ (ads) is rather strongly perturbed electronically in its adsorptive interaction with Al_2O_3.

The 1748cm^{-1} feature which forms extensively above ~ 250K is assigned as a polymer of $(HCO)_2$. It is well known that $(HCO)_2$ will polymerize

easily and Harris (34) has published an infrared spectrum of the polymer which coated his gas cell windows during IR studies of $(HCO)_2(g)$. Careful measurement of the literature spectrum indicate that ν_{CO} for this polymer was observed at 1747cm^{-1}, in good agreement with our feature on Al_2O_3 at 1748cm^{-1}.

Features in the C-H stretching region at 2930cm^{-1} and 2840cm^{-1} are assigned as polymer and monomer species respectively and their relative intensity changes on warming roughly parallel the ν_{CO} intensity changes. $(HCO)_2(g)$ exhibits ν_{CH}=2844cm^{-1} (34), in good agreement with this assignment, whereas the condensed polymer exhibits a weak C-H stretching mode at 2924cm^{-1} (34).

VII. SUMMARY

(1) The adsorption of H_2CO or $(HCO)_2$ on Rh/Al_2O_3 surfaces produces species having similiar infrared spectra in the carbonyl-stretching region. These species resemble chemisorbed CO at low coverages on crystalline Rh sites. However the $Rh(CO)_2$ species observed for CO adsorption on isolated Rh^+ sites are not readily produced from either H_2CO or $(HCO)_2$.

(2) No spectral evidence is found for the stabilization of chemisorbed HCO (or DCO) species on Al_2O_3-supported Rh when H_2CO, $(HCO)_2$, or atomic D+CO(ads) are used as potential sources of chemisorbed HCO (or DCO).

(3) Stable surface species are produced from the interaction of H_2CO or $(HCO)_2$ with Al_2O_3.

We conclude that quantities of HCO(ads) species cannot be stabilized by chemisorption on Rh surfaces or on Rh^+ sites present on Al_2O_3-supported

Rh, even at low temperatures. This observation suggests that mechanisms involving adsorbed hydrogen atom attack on chemisorbed CO to eventually produce hydrocarbon products may be unrealistic.

** The identification of specific suppliers and manufacturers is provided to aid the reader. No endorsement of this product by NBS is implied.

VIII. ACKNOWLEDGEMENTS

The authors would like to thank Dr. S. M. Girvin and Dr. T. M. Duncan for many profitable discussions. This work is partially supported by the Office of Naval Research, Contract N00014-81-F-0008

REFERENCES

1. (a) D. W. Goodman, R. D. Kelley, T. E. Madey, and J. T. Yates, Jr. J. Catal. 63, 226-234 (1980).
(also see earlier references therein to work on supported Ni which originally suggested a dissociative CO mechanism).
(b) For a recent review, see V. Ponec, Cat. Rev. Sci. Engr., 18, 151 (1978).

2. John G. Ekerdt and A. T. Bell, J. Catal., 58, 170 (1979).

3. J. A. Rabo, A. P. Risch and J. L. Poutsma, J. Catal. 53, 295 (1978).

4. R. A. Della Betta and M. Shelef, J. Catal., 48, 111 (1977); see also J. Catal., 60, 169 (1979).

5. B. A. Sexton and G. A. Somorjai, J. Catal., 46, 167 (1977).

6. D. G. Castner and G. A. Somorjai, Surf. Sci., 83, 60 (1979).

7. J. T. Yates, Jr., E. D. Williams, and W. H. Weinberg, Surf. Sci., 91, 562 (1980); see also D. G. Costner, L. H. Dubois, B. A. Sexton, and G. A. Somorjai, Surf. Sci., 103 (1981) L134.

8. E. L. Muetterties and J. Stein, Chem. Rev., 79, 479 (1979).

9. G. A. Mills and F. W. Steffgen, Catal. Rev., 8 (2), 159 (1973).

10. D. W. Goodman, T. E. Madey, M. Ono, and J. T. Yates, Jr., J. Catal., 50, 279 (1977).

11. J. T. Yates, Jr., T. E. Madey, and M. J. Dresser, J. Catal., 30, 260 (1973).

12. S. D. Worley and J. T. Yates, Jr., J. Catal., 48, 395 (1977).

13. (a) T. J. Collins and W. R. Roper, JCS Chem. Comm., p. 1044, (1976).
(b) R. L. Pruett, R. C. Schoening, J. L. Vidal, and R. A. Fiato, J. Organometallic Chem., 182, C57 (1979).
(c) J. A. Gladyz and J. C. Selover, Tetrahedron Letters, 4 319 (1978).

14. J. T. Yates, Jr. T. M. Duncan, S. D. Worley, and R. W. Vaughan, J. Chem. Phys., 70, 1219 (1979).

15. R. R. Cavanagh and J. T. Yates, Jr., J. Chem. Phys., accepted.

16. R. G. W. Norrish and G. A. Griffiths, Journal of the Chemical Society, 2829 (1928).

17. (a) R. G. Greenler, J. Chem. Phys. 37, 2094 (1962);
(b) J. D. Donaldson, J. F. Knifton and S. D. Ross, Spectrochimica ACTA 20, 847 (1964);
(c) Y. Noto, K. Fukuda, T. Onishi and K. Tamaru, Trans. Faraday Soc. 63, 2300 (1967);
(d) M. Ito and W. Syetake, J. Phys. Chem. 79, 1190 (1975).

18. R. R. Cavanagh and J. T. Yates, Jr., J. Chem. Phys., (accepted).

19. P. A. Thiel, E. D. Williams, J. T. Yates, Jr., and W. H. Weinberg, Surface Sci., 84, 199 (1979).

20. L. H. Dubois and G. A. Somorjai, Surface Sci., 91, 514 (1980).

21. J. T. Yates, Jr. S. D. Worley, T. M. Duncan, and R. W. Vaughan, J. Chem. Phys., 70, 1225 (1979).

22. E. D. Williams, P. A. Thiel, W. H. Weinberg, and J. T. Yates, Jr. J. Chem. Phys., 72, 3496 (1980).

23. R. R. Cavanagh and J. T. Yates, Jr., J. Catalysis, (in press).

24. G. E. Ewing, W. E. Thompson and G. C. Pimentel, J. Chem. Phys., 32, 927 (1960).

25. D. E. Milligan and M. E. Jacox, J. Chem. Phys., 41, 3032 (1964).

26. F. J. Adrian, E. D. Cochran and V. A. Bowers, J. Chem. Phys., 36, 1661 (1962).

27. D. E. Milligan and M. E. Jacox, J. Chem. Phys., 38, 2627 (1963).

28. C. P. Casey and S. M. Neumann, J. Amer. Chem. Soc., 98, 5395 (1976).

29. J. P. Collman and S. R. Winter, J. Amer. Chem. Soc., 95, 4089 (1973).

30. M. Primet and E. Garbowski, Chem. Phys. Letters, 72, 472 (1980).

31. A. N. Sidorov, Zh. fiz. khim. 30, 995 (1956).

32. V. Ya. Davydov, A. V. Kiselev, and B. D. Kuznetsov., Zh. fiz. khim. 39, 2058 (1965).

33. G. Herzberg, Molecular Spectra and Molecular Structure II. Infrared and Raman Spectra of Polyatomic Molecules. Van Nostrand Reinhold. Co. New York, (1945).

34. R. K. Harris, Spectrochim Acta 20, 1129 (1964).

FIGURE CAPTIONS

Fig. 1 Variable temperature infrared cell. The tungsten filament for dissociation of D_2 to atomic D is indicated, as is the radiation shield.

Fig. 2. Infrared spectrum of H_2CO adsorbed on Al_2O_3. The sample is dosed with formaldehyde while at 100K (a). Spectrum b-d indicate changes while warming to the indicated temperature. Spectrum (e) was recorded after evacuating the sample to $\sim 1.10^{-5}$ Torr.

Fig. 3. Infrared spectrum of H_2CO chemisorbed on Rh/Al_2O_3. (a)-(c) correspond to the spectral developments following introduction of H_2CO at 80K. Subsequent evacuation and saturation with CO resulted in spectrum (d).

Fig. 4. Perturbation of ^{13}CO (ads) on Rh/Al_2O_3 following exposure to H_2 $^{12}CO(g)$.

Fig. 5. Infrared spectrum of glyoxal $(HCO)_2$ adsorbed on Al_2O_3.

Fig. 6. Infrared spectrum of $(HCO)_2$ chemisorbed on Rh/Al_2O_3.

Fig. 7. Interaction of atomic deuterium with chemisorbed CO on Rh/Al_2O_3.

TABLE I

INFRARED FEATURES OBSERVED FOR H_2CO ADSORPTION ON Al_2O_3

(cm^{-1})

Sample Temperature (K)	<200	200-300	>300 +evacuation
	2977	2977	2962
	2913	2913	2908
	2788	2788	2788
	2040 (br)		
	1700	1770-1700	1770-1700
		1594	1594
		1392	1392
		1372	1372
	1470	1470	1470
	1430	1430	unresolved
	1395	1395	
	1280	1280	1300
	1230	1230	1230
	1150	1150	1150

TABLE II

INFRARED FREQUENCIES OBSERVED FOR THE HCO LIGAND

MOLECULE	Wavenumber (cm^{-1}) νC-H	νC=O	νHCO (bend)	REF
HCO (in CO matrix)	2488	1861	1090	25
$Os(HCO)\,Cl(CO)_2(PPh_3)_2$		1610		13(a)
$[Ir_4(CO)_{11}(HCO)]^-$		1590-1610		13(b)
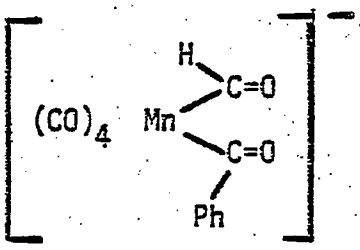		1588		13(c)
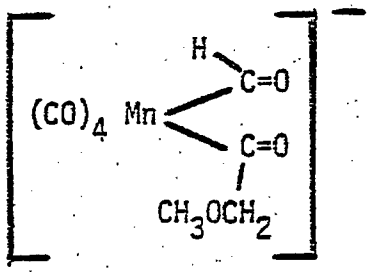		1604		13(c)
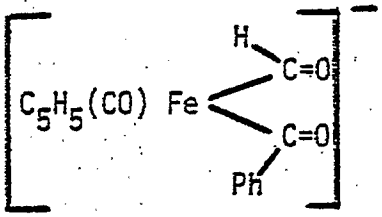		1555		13(c)
$[Et_4N]\,[(PhO)_3P]\,(CO)_3\,FeHCO$		1584		28
$[(CO)_4\,Fe\,(CHO)]^-$	2690 2540	1577-1610		29

Variable Temperature Infrared Cell

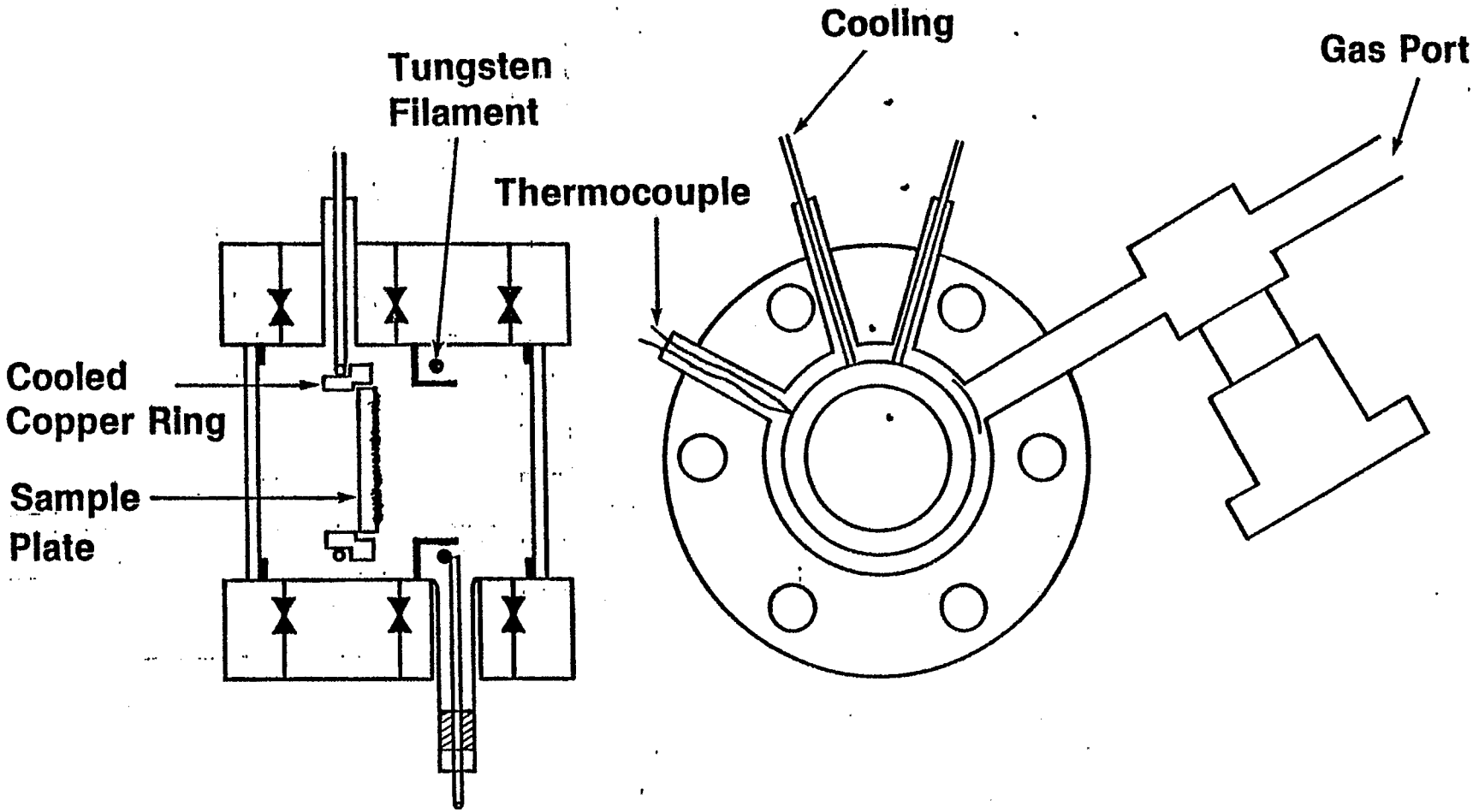

Figure 1

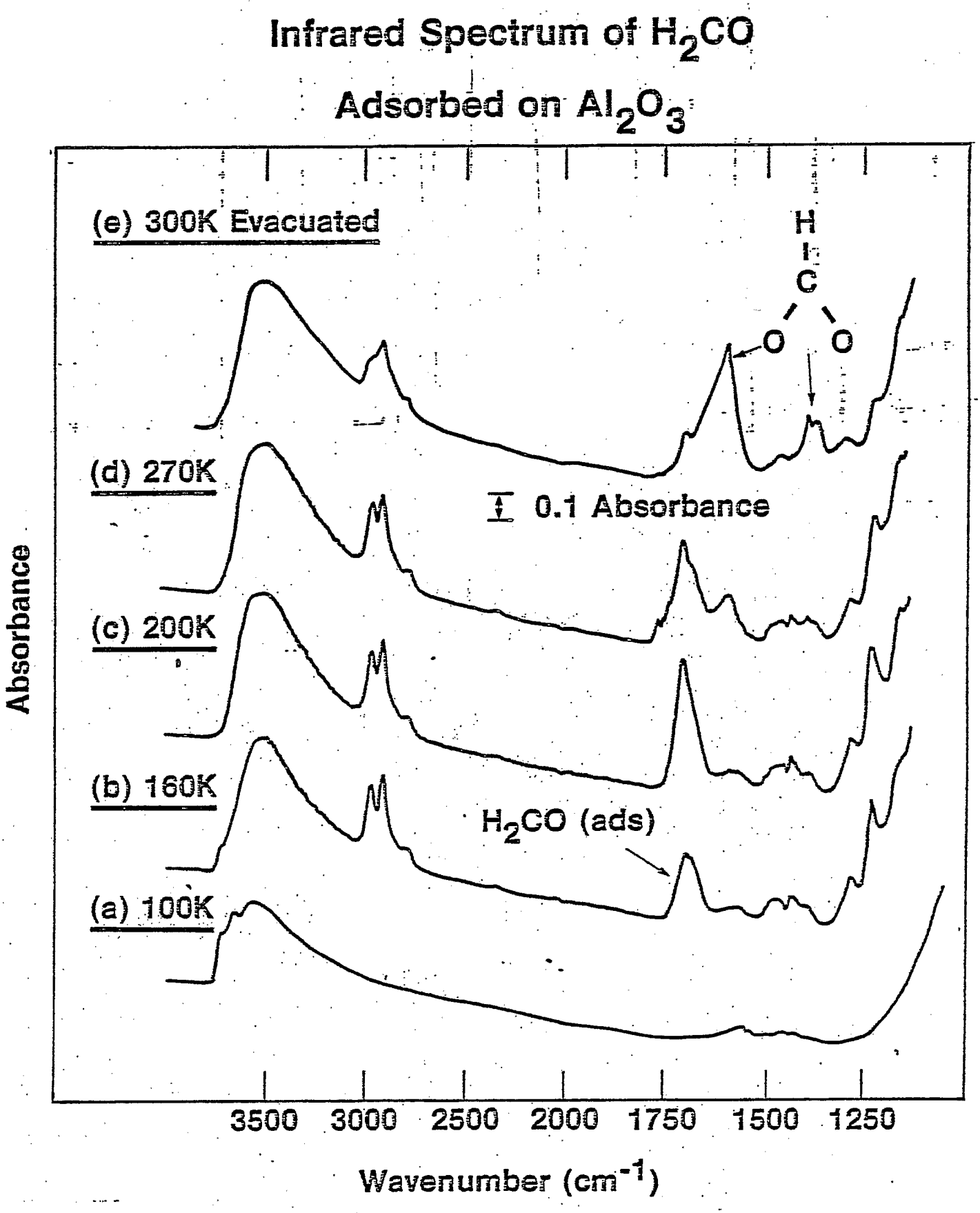
Infrared Spectrum of H_2CO
Adsorbed on Al_2O_3
(e) 300K Evacuated
H
C
O
O
(d) 270K
0.1 Absorbance
(c) 200K
(b) 160K
H_2CO (ads)
(a) 100K
Absorbance
3500
3000
2500
2000
1750
1500
1250
Wavenumber (cm^{-1})

Figure 2

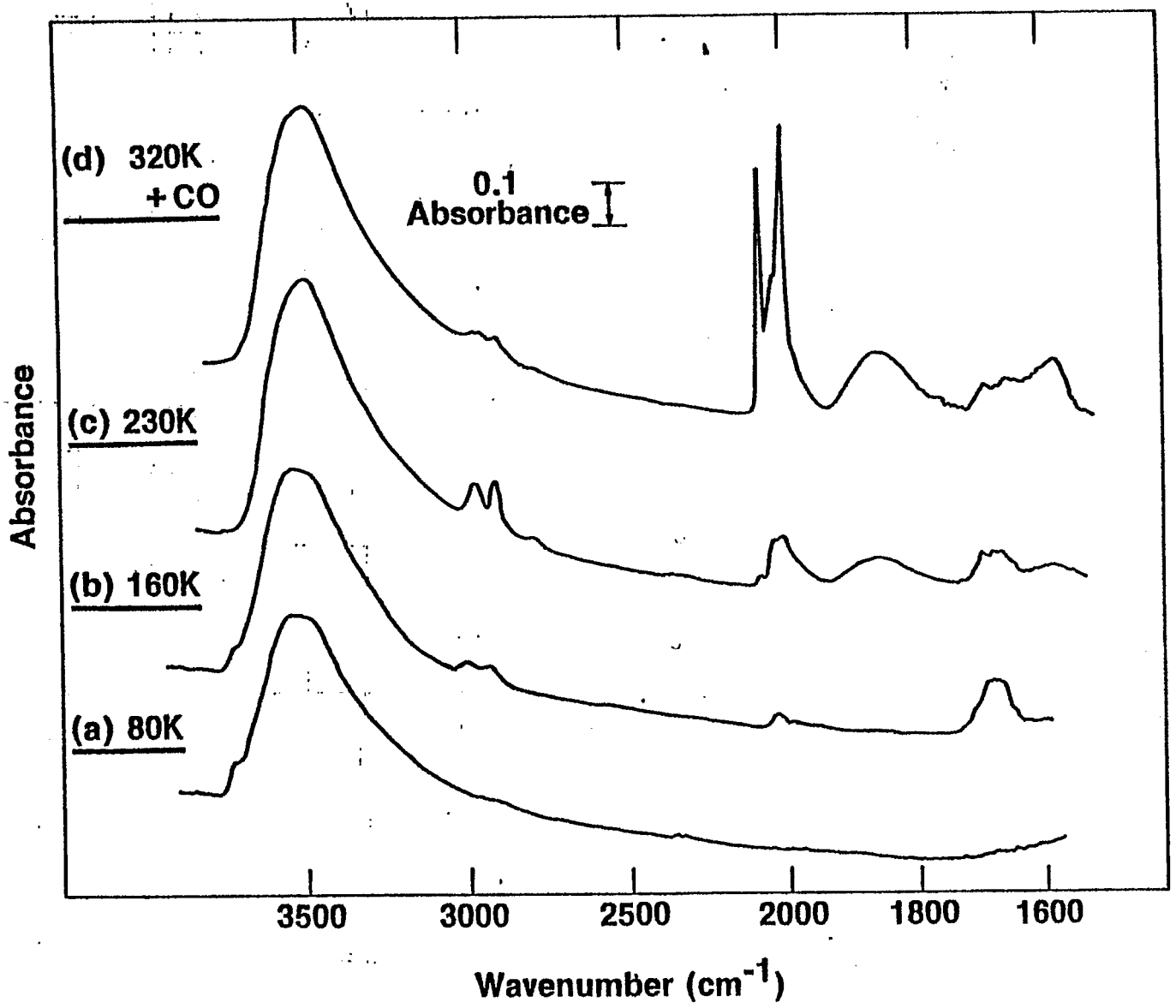
Infrared Spectrum of H_2CO
Chemisorbed on Rh/Al_2O_3
(d) 320K
+CO
0.1
Absorbance
(c) 230K
(b) 160K
(a) 80K
Absorbance
3500
3000
2500
2000
1800
1600
Wavenumber (cm^{-1})

Figure 3

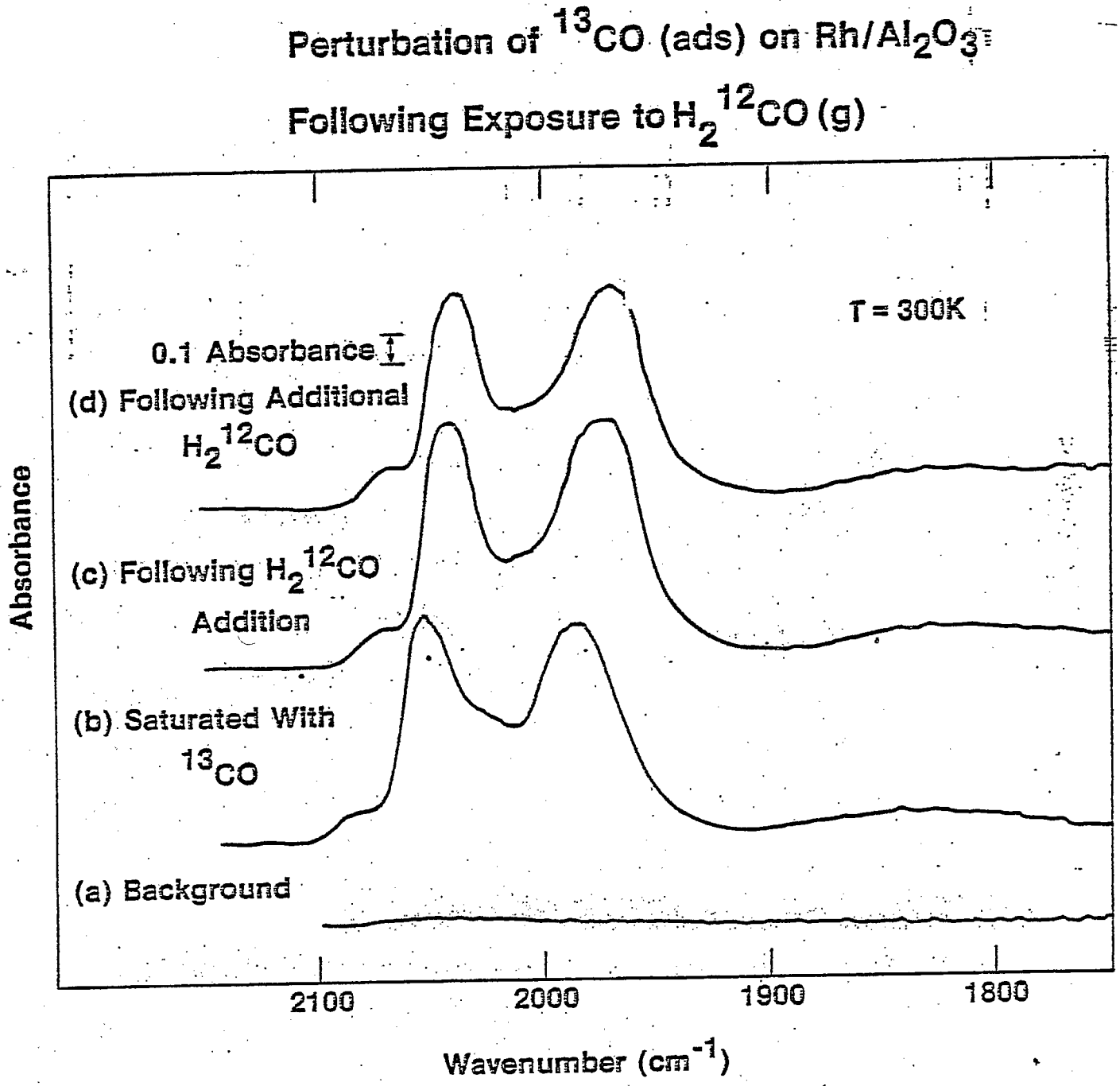
Perturbation of ^{13}CO (ads) on Rh/Al_2O_3
Following Exposure to H_2 ^{12}CO (g)
T = 300K
0.1 Absorbance
(d) Following Additional H_2 ^{12}CO
(c) Following H_2 ^{12}CO Addition
(b) Saturated With ^{13}CO
(a) Background
Absorbance
2100
2000
1900
1800
Wavenumber (cm^{-1})

Figure 4

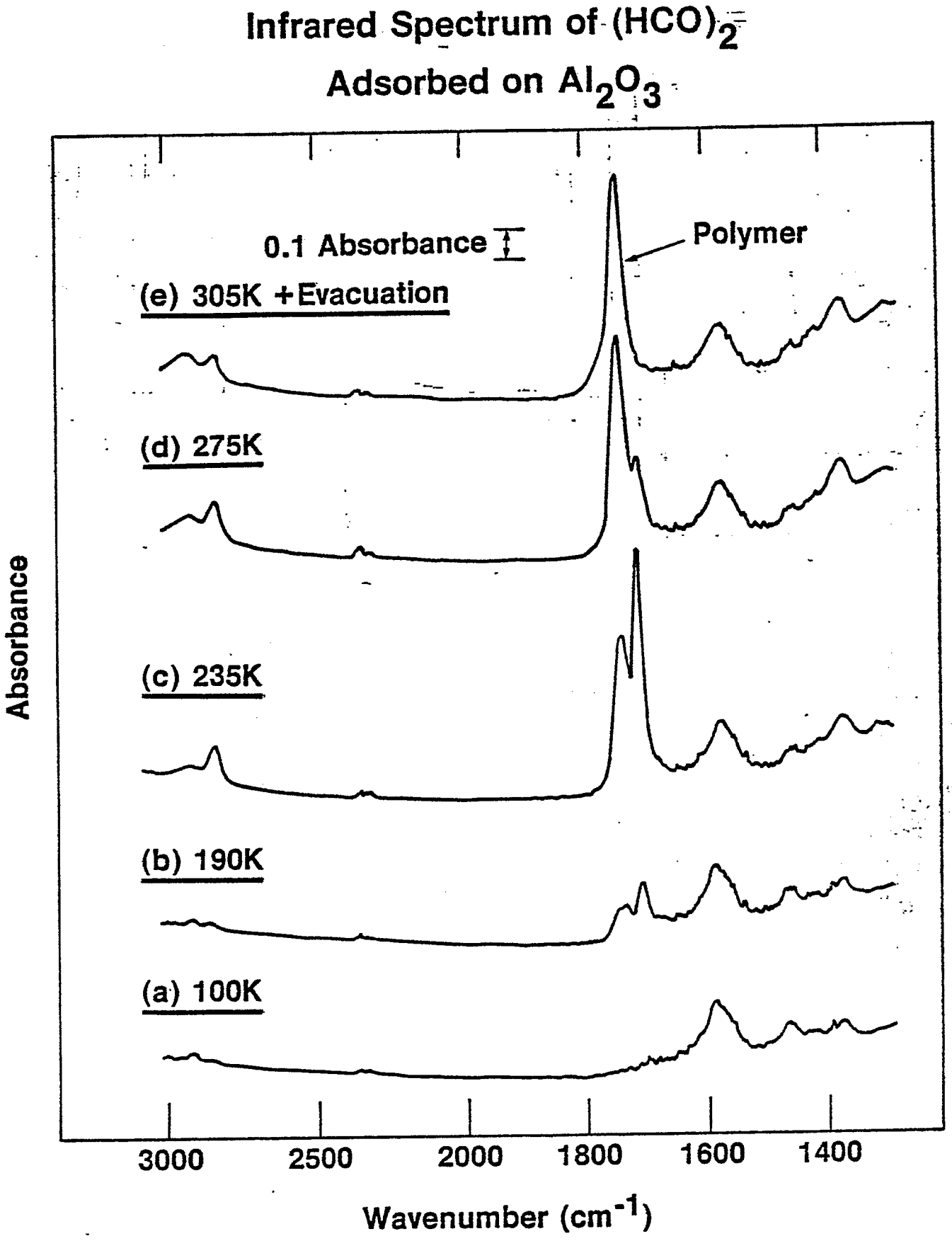
Infrared Spectrum of $(HCO)_2$
Adsorbed on Al_2O_3
0.1 Absorbance
Polymer
(e) 305K +Evacuation
(d) 275K
(c) 235K
(b) 190K
(a) 100K
Absorbance
3000
2500
2000
1800
1600
1400
Wavenumber (cm^{-1})

Figure 5

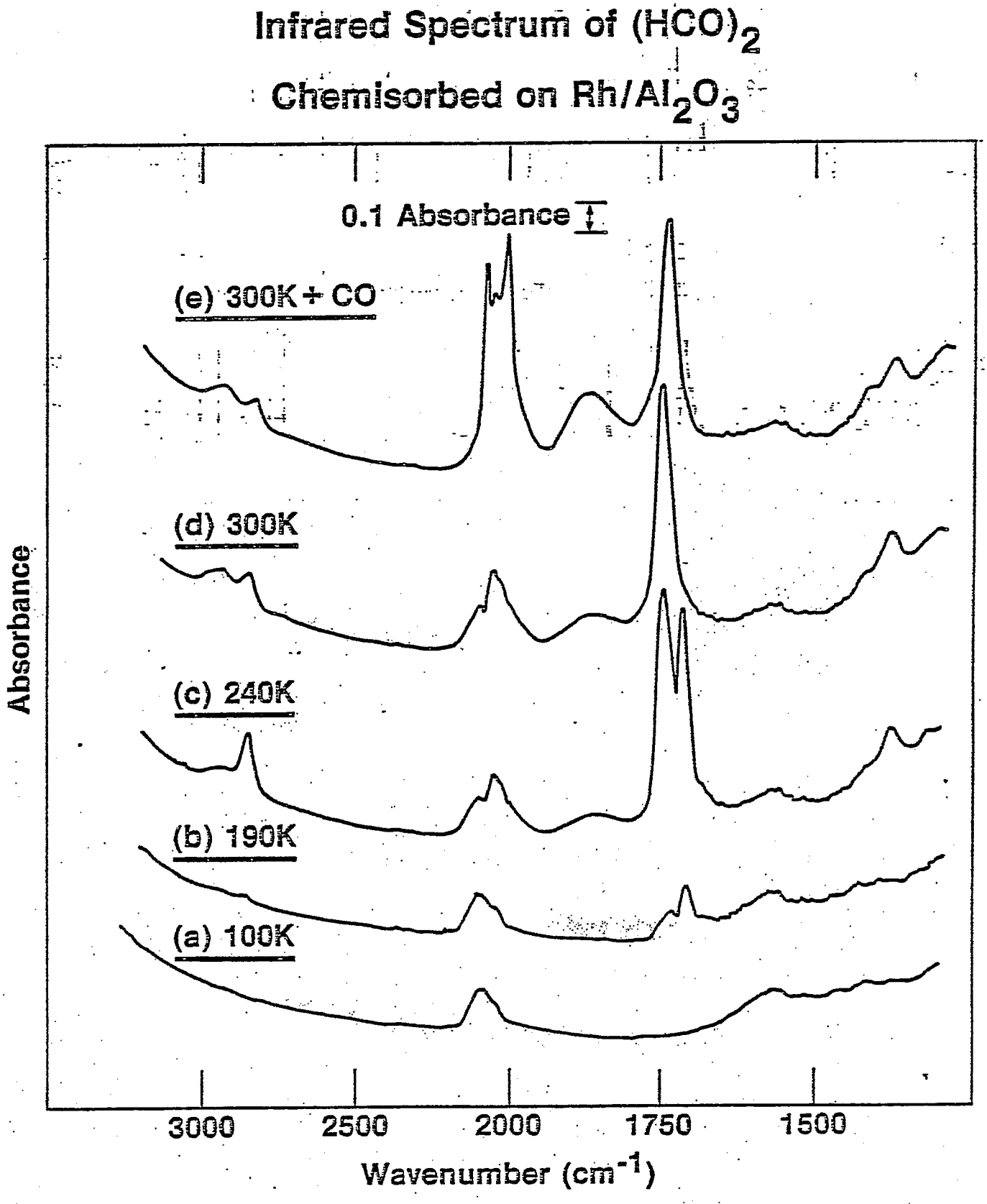
Infrared Spectrum of $(HCO)_2$
Chemisorbed on Rh/Al_2O_3
0.1 Absorbance
(e) 300K + CO
(d) 300K
(c) 240K
(b) 190K
(a) 100K
Absorbance
3000
2500
2000
1750
1500
Wavenumber (cm^{-1})

Figure 6

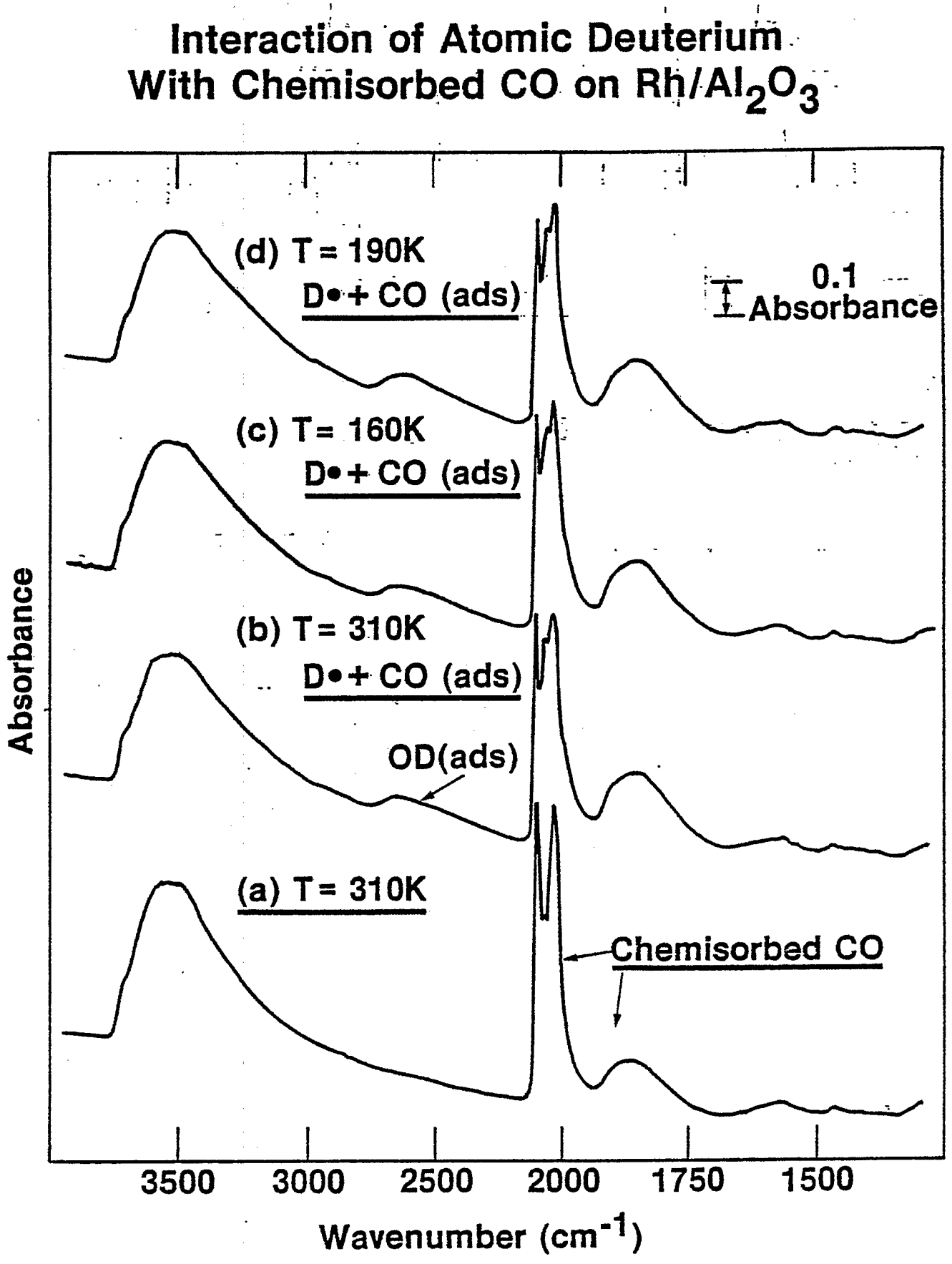
Interaction of Atomic Deuterium
With Chemisorbed CO on Rh/Al2O3
(d) T = 190K
D• + CO (ads)
0.1
Absorbance
(c) T = 160K
D• + CO (ads)
(b) T = 310K
D• + CO (ads)
OD(ads)
(a) T = 310K
Chemisorbed CO
Absorbance
3500
3000
2500
2000
1750
1500
Wavenumber (cm-1)

Figure 7